Interactions between grain size and composition of sediments: two examples

H. von Eynatten[1], R. Tolosana-Delgado[2], S. Triebold[1], T. Zack[3]
[1] GZG, Universität Göttingen, Germany: hilmar.von.eynatten@geo.uni-goettingen.de
[2] IMA, Universitat de Girona, Spain, [3] Mineralogisches Institut, Universität Heidelberg, Germany

Abstract

Two contrasting case studies of sediment and detrital mineral composition are investigated in order to outline interactions between chemical composition and grain size. Modern glacial sediments exhibit a strong dependence of the two parameters due to the preferential enrichment of mafic minerals, especially biotite, in the fine-grained fractions. On the other hand, the composition of detrital heavy minerals (here: rutile) appears to be not systematically related to grain-size, but is strongly controlled by location, i.e. the petrology of the source rocks of detrital grains. This supports the use of rutile as a well-suited tracer mineral for provenance studies. The results further suggest that (i) interpretations derived from whole-rock sediment geochemistry should be flanked by grain-size observations, and (ii) a more sound statistical evaluation of these interactions require the development of new tailor-made statistical tools to deal with such so-called two-way compositions.

Kew words: ANOVA, biplots, clr-transformation, granulometry, log-linear modelling

1 Introduction

Grain-size distribution belongs to the most important physical properties of sediments and sedimentary rocks. Grain size exerts strong control on the petrographic and chemical composition of sediments, because chemical alteration and mechanical breakdown of source rocks, followed by sorting of particles during transport and deposition, lead to preferential enrichment of specific materials in certain grain-size fractions (e.g., Weltje and von Eynatten, 2004). In this paper, we preliminarily evaluate the interaction between sediment grain size and chemical composition in two strongly contrasting examples: (1) whole-rock chemistry of modern glacial sediments, and (2) mineral chemistry of individual rutile grains from modern sands as well as two Paleozoic sandstones.

In statistical terms, both examples call for an assessment of the dependence or independence of mineral or sediment composition with respect to grain size. Classical techniques to apply in this case are equality-of-means tests (or ANOVA tests) and box-plots. Equality-of-means test assesses the homogeneity of the mean of a variable between two groups, whereas ANOVA models do the same for several groups; these models are built under the hypothesis that these means follow a normal distribution with identical variance. To increase the credibility of such hypothesis, a logarithm or a centered log-ratio transformation may be applied to the data set. Independently, a series of biplots of the transformed components with respect to the grain size may help to assess the homogeneity of the covariance structure. This study serves as a first step towards a more comprehensive and quantitative understanding of the interdependence of sediment grain-size distribution and chemical composition.

2 Data set description

To study interactions between grain size and geochemistry, the ideal situation would be to deal with two-way compositions. As (one-way) compositions can be seen as vectors of positive elements where each component informs of the relative importance of a part in a whole, *two-way compositions* are matrices of positive elements where each component informs of the relative importance of the combination of two parts from two different criteria to split the whole. In our case, we would like to split it by grain-size classes, and afterwards, analyze the chemical composition of the material in each grain-size class. The arrangement of these measurements in a matrix would give a two-way composition.

Unfortunately, proper *true* two-way compositions have not yet been found in the literature, because most examples suffer from low or missing grain-size resolution or are inappropriate for a pilot study due to complex multiple process control on composition. Instead, we use two well-documented examples where some information about grain size was encoded in a variable, so that each (one-way) composition can be assigned to a specific grain-size class.

2.1 First example: glacial sediment

The composition of glacial sediments is expected to be mainly controlled by physical weathering, since low temperature and especially the scarcity of fluids strongly slow down chemical reactions. Nesbitt and Young (1996) presented a set of geochemical major element compositions from 48 sediment samples deposited in the Guys Bight Basin, Arctic Canada. These sediments are mainly derived from glacial erosion of high-grade metamorphic rocks, and subsequently sorted by fluvial transport under arctic climate conditions. The grain-size classes investigated comprise mud, silt to fine sand, medium sand, and coarse sand to gravel. Due to the different physical properties of the mineral phases involved (here: mainly quartz, feldspar, biotite, and garnet), each phase is expected to be preferentially enriched in certain grain-size fractions, which implies that each grain-size class investigated should have a distinct mineral content, and, hence, a distinct chemical composition.

2.2 Second example: detrital rutile grains

Rutile belongs to the most stable heavy minerals in clastic sediments, which makes it a good candidate as a tracer in provenance studies of sediments. Although its chemical formula is usually described as pure TiO_2, it contains significant amounts of trace elements (e.g., Cr, V, Fe, Nb, W, Zr, U) that can be precisely measured by electron microprobe or laser-ablation ICP-MS. These trace element characteristics can be used to reconstruct source rock petrology of detrital rutile grains (Zack et al., 2004a). Because rutile may occur in several grain-size fractions of the sediment, we need to evaluate if the choice of the rutile grain size is crucial to the trace-element geochemistry of the analyzed rutiles. We have chosen seven samples (called here *locations*) from different tectonic and metamorphic settings (EGB – Erzgebirge / Germany, 1 sample; EY – Central Alps / Switzerland, 3 samples; plus three samples from Upstate New York: Ad – Adirondack/Gloversville, Cat – Catskill and Sha – Shawangunk). The first 5 samples are modern sands, the latter two are Paleozoic sandstones. The data are taken from Zack et al. (2004a) and Triebold et al. (unpublished data). We have analyzed in total approximately 750 individual rutile grains (each one being referred as a *sample*) that cover the two most prominent grain-size fractions containing detrital rutile for each sample (63-125 and 125-250 μm).

3 Methodology: comparing differences on the means

One of the most basic tests in statistics is equality-of-means, explained in most textbooks. Let X_1 and X_2 be two random variables with normal distributions $\boldsymbol{N}(\mu_1, \sigma_1^2)$ and $\boldsymbol{N}(\mu_2, \sigma_2^2)$, with unknown parameters. In general, we may have a variable split by *groups*: $X_i \sim \boldsymbol{N}(\mu_i, \sigma_i^2)$, with $i=\{1,2,\ldots,N\}$, with each i defining a group. Given a sample of size n_i for the i-th group, $\bar{x}_i$ and s_i^2 may represent the maximum-likelihood estimators of the mean and the variance of this group. Then, the pooled sample size, mean and variance are

$$n_p = n_1 + n_2 = \sum n_i\,, \qquad \bar{x}_p = \frac{n_1\bar{x}_1 + n_2\bar{x}_2}{n_p} = \frac{\sum n_i\bar{x}_i}{n_p}\,, \qquad s_p^2 = \frac{n_1 s_1^2 + n_2 s_2^2}{n_p} = \frac{\sum n_i s_i^2}{n_p}\,. \tag{1}$$

The variance s_p^2 is also called *intra-group variance*, especially when we work with more than two groups. In this case, an *inter-group variance* is also defined, and its experimental version is computed as the moment of inertia of each group mean with respect to the pooled mean

$$s_x^2 = \frac{\sum n_i\left(\bar{x}_i - \bar{x}_p\right)^2}{n_p}\,. \tag{2}$$

Assume all groups to have the same population variance: $\sigma^2 = \sigma_1^2 = \sigma_2^2 = \cdots = \sigma_N^2$. Then, it can be estimated with the intra-group variance, s_p^2, which as a random variable follows a χ^2 distribution with $\nu = n_p - N$ degrees of freedom. Then we can build a test on the equality of means of group i and j. We take

as null hypothesis equality of these means $\{\mu_i = \mu_j\}$, and as alternative hypothesis difference on these means $\{\mu_i \neq \mu_j\}$. Under the null hypothesis, the statistic

$$\hat{t} = \frac{\bar{x}_i - \bar{x}_j}{s_p \sqrt{\frac{1}{n_i} + \frac{1}{n_j}}} \sim t\left(n_i + n_j - 2\right) \tag{3}$$

allows us to compute a p-value of the null hypothesis by computing the probability of a Student's *t* distribution above the experimental value $\tilde{t}$. Recall that a hat represents an estimator (=a random variable), and a tilde an estimate (=a number). In this way, we may compare the means of as many groups as we want, but always by pairs. An alternative global approach can be obtained when comparing the *intra-group* (1) and *inter-group* (2) variances, which evolves into the so-called ANalyis Of VAriance models (ANOVA). However, we have not fully followed this approach and it is therefore not explained (see, e.g., Simonoff, 2003, for a good general account).

Note that these techniques are based upon normality of the variable. In fact, this normality is only needed for the means, and the central limit theorem ensures us this normality for *big* samples. But for *small* samples, it is wise to check normality of the original variable. Considering our data as compositions, it seems reasonable to take a log-ratio transformation, so that the transformed scores may better follow such a normal distribution. From the available transformations, we have chosen the well-known centered log-ratio transformation (Aitchison, 1986)

$$\mathrm{clr}_i(\mathbf{x}) = \ln \frac{x_i}{g(\mathbf{x})}, \tag{4}$$

where $\mathbf{x} = [\, x_1, x_2, \ldots, x_D]$ is a vector representing the composition. Finally, note in passing that no consideration has been made with regard to experimental errors: sample sizes are considered big enough as to neglect their possible effects.

4 Results and Discussion

4.1 First example: glacial sediment

Figure 1 shows a biplot (Gabriel, 1971) of the clr-transformed data set (a compositional biplot, as defined by Aitchison, 1997), distinguished by grain-size classes. It is easy to see a preferential enrichment of the finer grain sizes (1-2, mud to fine sand) in *mafic* oxides (Fe, Ti, Mg, P), whereas *felsic* oxides (Si, Al, K, Na) are relatively enriched in coarser grain sizes (3-4, medium sand to gravel). We also see a heterogeneous spread of each grain size. These aspects might indicate that the variance-covariance structure is not homogeneous among grain sizes. However, the number of samples in each group is too small to generate significant separate biplots. We assume this homogeneity of variance without any test.

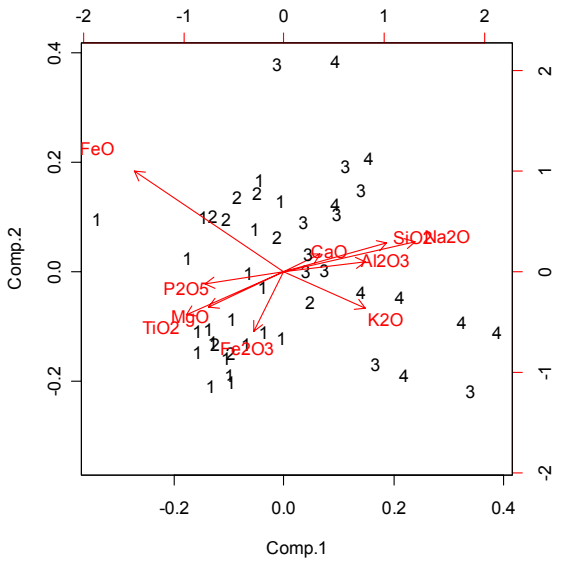

Figure 1: Biplot (85.6% of explained variability) of sediment composition, distinguishing samples according to their grain size: 1-mud, 2-silt to fine sand, 3-medium sand, and 4-coarse sand to gravel. There are not enough individuals in each of these grain sizes as to allow a meaningful representation of the separate biplots.

Figure 2 offers a graphical comparison of the clr-means of each part distinguishing among grain sizes. The relative association of felsic and mafic oxides with coarse and fine grain-size fractions is again clearly visible. Furthermore, we can detect a clear trend of progressive enrichment in Si, Al and Na oxides, and depletion of Ti and Mg oxides as grains become coarser. A related linear trend using non-centred principal component analysis within an amalgamated three-part simplex (Al_2O_3, $CaO+Na_2O+K_2O$, $FeO+MgO$) was already described by von Eynatten (2004). The rest of the elements show also important differences between mud (class 1) and gravel (class 4), but the trend is not clearly monotonic. Surprisingly, neither Fe_2O_3 nor FeO follow this trend, as could be expected from the strong association of iron with biotite and heavy minerals. Figure 3 shows the trend of the clr-transformed total $Fe_{(tot)} = 0.90 \cdot Fe_2O_3 + FeO$ (classical amalgamation), which is more consistent with our expectations. The comparison of all the iron box-plots (Figures 2 and 3) suggests a slightly positive anomaly in the ratio FeO/Fe_2O_3 for the second grain-size class which distorts the monotonically-decreasing trend expected for these two species. This observation is tentatively assigned to the possible enrichment of garnet in silt and fine sand. Once detected this anomaly, we switch back to the full composition (distinguishing between Fe species) to proceed with tests on the mean.

In the box-plots of Figure 2 individual boxes are notched: these notches represent a 95% (asymptotically-valid) confidence interval around the median (McGill et al, 1978) *when the samples have equal size*. Thus, if two notches overlap, the corresponding medians are not different enough at the 5% level. Therefore, as a general idea, 1 (mud) and 2 (silt to fine sand) are generally not distinguishable (except for Fe_2O_3), whereas grain-size classes 3 (medium sand) and 4 (coarse sand to gravel) are only different in their content of Al_2O_3, Fe_2O_3 and K_2O. These two groups (1 and 2 vs. 3 and 4) are then significantly different in their general chemistry (except by K_2O, both Fe species, and maybe MgO).

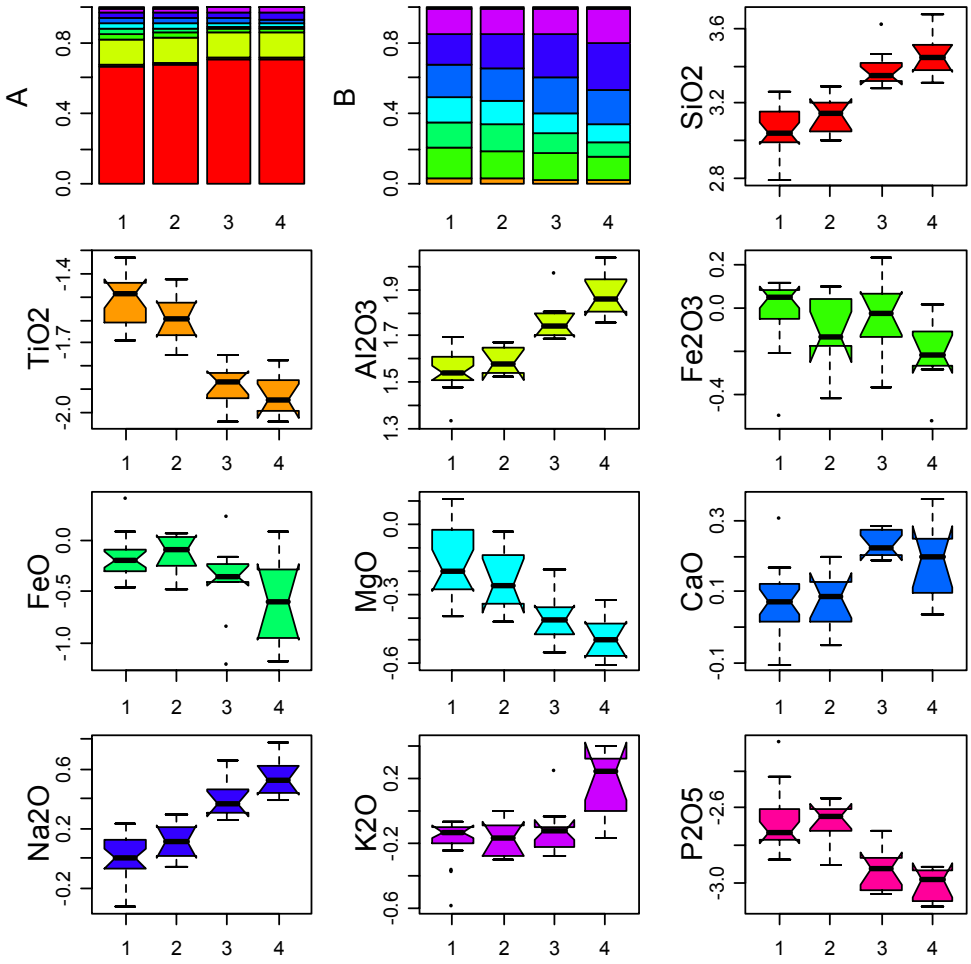

Figure 2: Barplots and boxplots of the glacial sediment composition: (A) barplot of the geometric mean composition of each grain size (from SiO_2 to P_2O_5). (B) barplot of the geometric mean subcomposition of each grain size, discarding SiO_2 and Al_2O_3. (Others) boxplots of each clr-transformed major element oxide, distinguished by grain-size classes 1 to 4 (1-mud, 2-silt to fine sand, 3-medium sand, and 4-coarse sand to gravel); boxplots are notched, to approximately represent a 95% confidence interval on the median. Note that colors of the boxplots act as legend for the barplots.

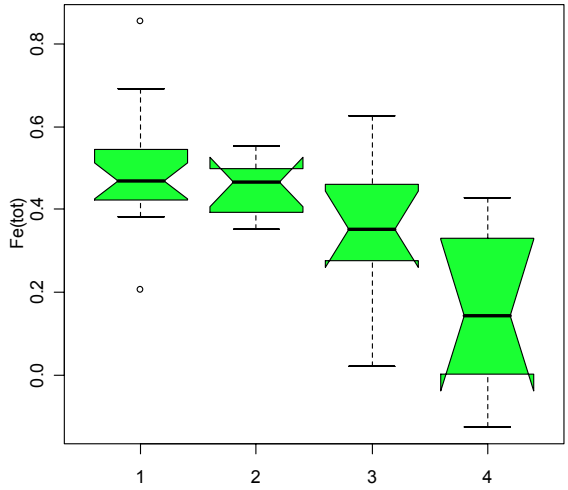

Figure 3: Box-plot of clr-transformed total iron $Fe_{(tot)}$. The other boxplots and barplots in Figure 2 do not significantly change when Fe_2O_3 and FeO are replaced by $Fe_{(tot)}$. Recall that the notch represents a 95% confidence interval on the median. Note that there is a clear trend from mud to gravel, although the notches of two consecutive boxes coincide, thus there is no strict indication of difference in the median/mean. Codes of grain sizes: 1-mud, 2-silt to fine sand, 3-medium sand, and 4-coarse sand to gravel.

These differences are tested in Table 1, which shows the significance of some tests of equality of the mean. These tests take as null hypothesis equality of the means in the first and *i*-th group, against the alternative hypothesis of difference on these means. These tests assume the same variance for all groups. Table 1 only reports the bilateral p-values attached to these tests. From column 2, one can conclude that there is no important difference between mud (class 1) and silt to fine sand (class 2) grain sizes (except for TiO_2 and Na_2O, possibly), whereas both medium sand (class 3) and coarse sand to gravel (class 4) are strongly different to mud. Finally, classes 3 and 4 are clearly different in K_2O, and may be accepted to be different also in Al_2O_3, Fe_2O_3, MgO and Na_2O.

Table 1. Bilateral p-values of the null hypothesis (1st to 4th columns: with pooled variance from groups 1 to 4; 5th column: with pooled variance only using groups 3 and 4). The stars show those p-values smaller than: 0.1(*), 0.05(**) and 0.01(***). Sub-indices of the means relate to grain size: 1-mud, 2-silt to fine sand, 3-medium sand, and 4-coarse sand to gravel.

	$\mu_1=0$ vs $\mu_1\neq 0$		$\mu_2=\mu_1$ vs $\mu_2\neq\mu_1$		$\mu_3=\mu_1$ vs $\mu_3\neq\mu_1$		$\mu_4=\mu_1$ vs $\mu_4\neq\mu_1$		$\mu_3=\mu_4$ vs $\mu_3\neq\mu_4$	
clr(SiO_2)	$2.4\cdot10^{-55}$	***	$1.2\cdot10^{-01}$		$2.8\cdot10^{-09}$	***	$1.2\cdot10^{-10}$	***	$1.80E^{-01}$	
clr(TiO_2)	$1.2\cdot10^{-44}$	***	$7.8\cdot10^{-02}$	*	$4.3\cdot10^{-12}$	***	$1.6\cdot10^{-12}$	***	$3.33E^{-01}$	
clr(Al_2O_3)	$6.9\cdot10^{-49}$	***	$2.5\cdot10^{-01}$		$2.0\cdot10^{-08}$	***	$2.6\cdot10^{-12}$	***	$1.91E^{-02}$	**
clr(Fe_2O_3)	$9.5\cdot10^{-01}$		$1.3\cdot10^{-01}$		$5.4\cdot10^{-01}$		$3.2\cdot10^{-03}$	***	$4.97E^{-02}$	**
clr(FeO)	$2.4\cdot10^{-02}$	**	$8.3\cdot10^{-01}$		$3.5\cdot10^{-02}$	**	$9.5\cdot10^{-04}$	***	$3.39E^{-01}$	
clr(MgO)	$1.9\cdot10^{-06}$	***	$1.5\cdot10^{-01}$		$1.7\cdot10^{-05}$	***	$3.5\cdot10^{-07}$	***	$9.32E^{-02}$	*
clr(CaO)	$2.5\cdot10^{-03}$	***	$6.8\cdot10^{-01}$		$7.2\cdot10^{-06}$	***	$1.6\cdot10^{-03}$	***	$1.93E^{-01}$	
clr(Na_2O)	$7.4\cdot10^{-01}$		$6.6\cdot10^{-02}$	*	$4.0\cdot10^{-09}$	***	$4.8\cdot10^{-12}$	***	$2.63E^{-02}$	**
clr(K_2O)	$3.0\cdot10^{-06}$	***	$9.7\cdot10^{-01}$		$2.6\cdot10^{-01}$	***	$1.2\cdot10^{-06}$	***	$3.57E^{-03}$	***
clr(P_2O_5)	$3.7\cdot10^{-50}$	***	$9.1\cdot10^{-01}$		$5.8\cdot10^{-06}$	***	$1.4\cdot10^{-07}$	***	$1.10E^{-01}$	

4.2 Second example: detrital rutile

The rutile trace element data set contains a significant amount of missing values (below detection limit, i.e. rounded zeroes), which should be either filtered or replaced for statistical evaluation. Comparing the biplots of the log-transformed data for both treatments (Figure 4), the impact of these treatments is clearly high. For this reason, we will conduct the analysis with both data sets: the replaced (replacing missing values by half the detection limit of that specific trace element) and the filtered (erasing the observations containing missing values). These plots also show which elements (Cr and Zr) are most distorted by the different data handling since: (i) missing values tend to cluster at the opposite side of these two elements,

and (ii) the relative position of the rest of the rays (V, W, Nb, Fe) barely changes. We decided to use the logarithmic transformation in this analysis instead of the clr-transformation, because: a) missing values are abundant, b) analyzed elements are present in small traces, c) so we can disregard the computation of the residual part, and the geometric mean of parts involved in the clr-transformation, d) logs are easier to interpret, but nevertheless e) they are numerically pretty similar. The appendix contains the same biplots of figure 4, obtained with clr-transformed data and log-transformed data, to demonstrate the degree of similarity between them (figure 7).

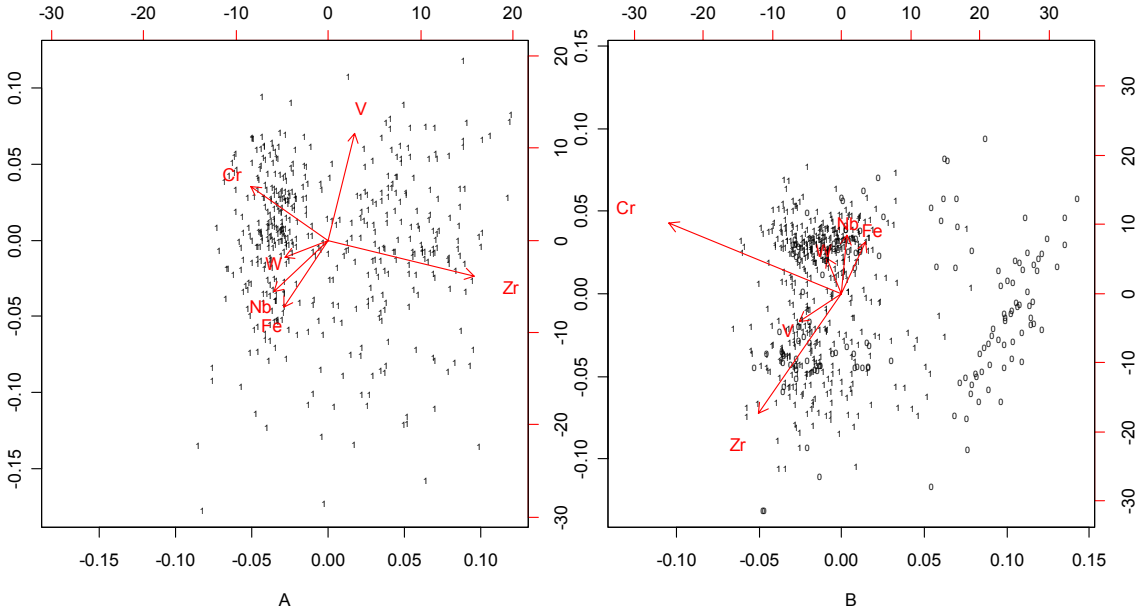

Figure 4: Biplots of the whole rutile data set: (A) filtering the missing values; (B) replacing the missing values by half of its detection limit. Missing values are marked with "0", whereas fully observed compositions with "1".

Table 2. Bilateral p-values of the null hypothesis in the equality-of-means tests. The stars show those p-values smaller than: 0.1(*), 0.05(**) and 0.01(***). Tests are applied on the data after replacing missing values by half of the detection limit, and by filtering the samples with missing values. Geometric means (in ppm) of the components are included, for coarse (C) and fine (F) grain sizes; p-values have been computed for equality of the logarithmic mean of the elements.

	%replaced	filtered				replaced			
	or filtered	mean C	mean F	p-value		mean C	mean F	p-value	
V	4.47	238.02	177.55	$7.88 \cdot 10^{-04}$	***	228.14	169.50	$1.55 \cdot 10^{-04}$	***
Cr	9.77	966.94	896.50	$3.50 \cdot 10^{-01}$		689.59	540.93	$3.71 \cdot 10^{-02}$	**
Fe	0.83	1659.42	1740.67	$5.31 \cdot 10^{-01}$		1706.36	1621.15	$4.95 \cdot 10^{-01}$	
Zr	5.30	277.38	258.11	$4.82 \cdot 10^{-01}$		228.14	201.05	$2.15 \cdot 10^{-01}$	
Nb	0.33	1925.01	2050.85	$4.47 \cdot 10^{-01}$		1887.38	1716.86	$2.33 \cdot 10^{-01}$	
W	39.40	112.30	146.33	$8.72 \cdot 10^{-04}$	***	97.34	110.26	$7.27 \cdot 10^{-02}$	*

The grain size information of this data set discriminates only between coarse (125-250µm) and fine (63-125µm) rutile grains. The mean trace composition (geometric average in ppm) for each of these two grain sizes is included in Table 2, with a p-value of a test of equality of these means (null hypothesis of equality of log-means, against alternative hypothesis of difference between the log-means, assuming homogeneous logarithmic variance for all groups). Clearly, only W and V may be taken as different between the two sets.

However, there are several populations mixed in this data set. Specifically, grains have been analyzed from different tectonic and metamorphic settings (EGB – Ergebirge / Germany; EY – Central Alps / Switzerland; and Catskill, Shawangunk and Adirondack samples from Upstate New York), including both modern sands and Paleozoic sandstones. Thus, a separate comparison should be done in this case, given that we have enough analyses of rutile geochemistry from each location. Figure 5 compares the geometric means obtained for each one of these seven locations, distinguishing grain size and missing value treatment. It is worth noting that the missing value treatment does not seem to have a strong influence,

except at Catskill location. Although this plot offers a rather bad visual assessment of the effects of grain size, one can say that the ratios V/Fe (filtered) or Cr/Fe (replaced) may distinguish grain sizes at Catskill. At Adirondack, Nb and/or Fe may distinguish between the two grain-size classes, and the fine-grained rutiles from Shawangunk seem poorer in W, V and Zr and richer in Fe compared to coarse ones from the same location. The samples obtained from the European Alps and Erzgebirge locations are remarkably more homogeneous, with a slight difference in Cr content in the EGB location. This may be due to the fact that the North-American samples represent larger drainage areas implying a higher possibility of mixing rutile from different sources having certain grain-size preferences.
A more meaningful comparison is given in Table 3, where tests of equality of the mean (like that of table 2) are independently conducted at each location. Instead of doing a joint analysis of the variance, we decided to do independent equality-of-means tests, because in our opinion, the noise introduced by the missing values blurs the intra-groups variance structure. Conducting separate tests seems more robust than pooling all group variances together. The most interesting feature of this table is the fact that Fe is never considered to be a discriminant component (Nb only once for filtered data set at EY-29-2), whereas V and Zr are the elements which most often display a significant difference between the two grain sizes (both of them in Catskill, Shawangunk and EGB-04-S50 locations; V also in Adirondack and Zr in EY-29-4). Cr has an important discriminating contribution at location EGB-04-S50, while W is selected as discriminant at EY-29-3 and EY-29-4 locations.

Finally, Figure 6 offers another graphical approach to these data sets: it compares through notched box-plots all seven locations and two grain sizes, for each of the six trace elements. It is clearly seen that, with the notable exception of V, differences among locations are much more important than differences between grain sizes. We see again that variability at North-American locations (Adirondack, Catskill and Shawangunk) is generally larger than variability at the European ones (EGB and EY samples), since box-plots of the former are generally wider than those of the former. Bar-plots show that only Adirondack and Catskill samples seem to have a different total amount of trace elements as a function of grain size. A striking contrast is observed for Zr-content of the Alpine samples (EY) which is much lower compared to all the other samples. This is related to the lower metamorphic grade of their host rocks compared to the granulite grade of EGB and North-American samples and confirms the Zr-geothermometer recently developed by Zack et al. (2004b).

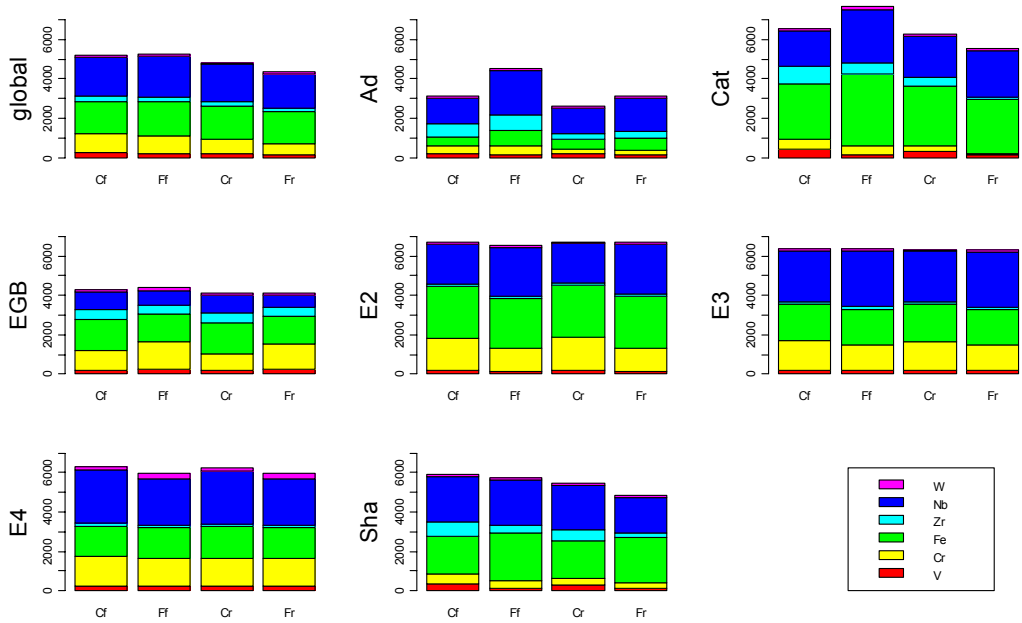

Figure 5: Barplots of the geometric means for every sample (location), distinguishing grain size and missing value treatment: Cf-coarse grains, filtering of missing values; Ff- fine grains, filtering; Cr-coarse grains, replacement; Fr-fine grains, replacement. Locations abbreviated according: (Ad)-Adirondack; (Cat)-Catskill; (Sha)-Shawangunk; (EGB)-EGB-04-S50; (E2)-EY-29-2; (E3)- EY-29-3; (E4)- EY-29-4. Vertical scale of barplots is ppm (cumulative).

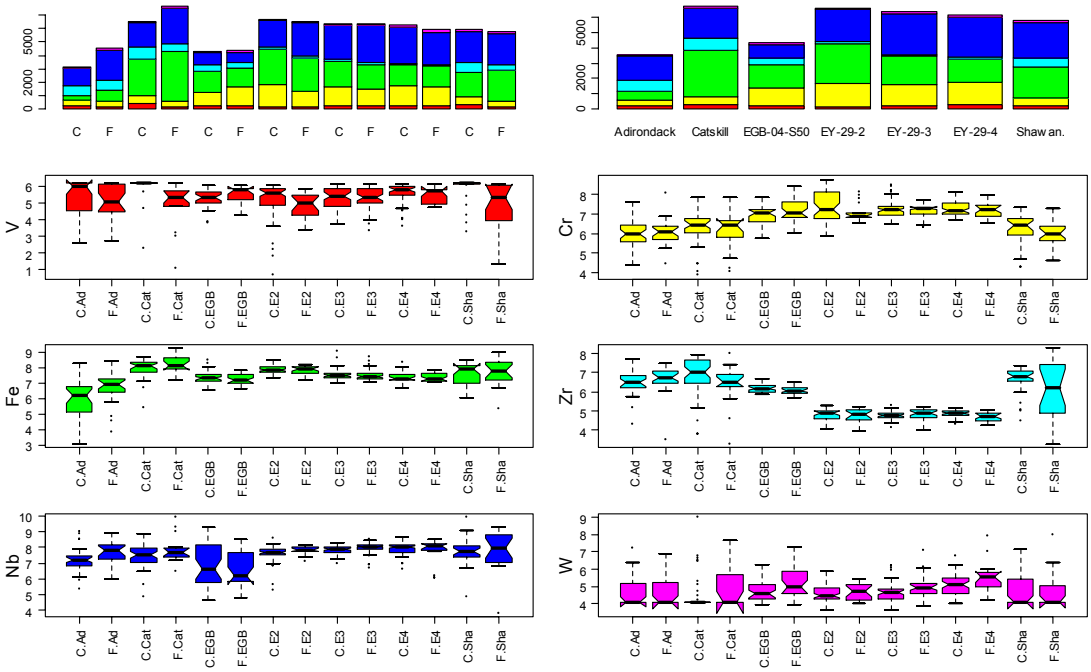

Figure 6: Barplots and boxplots of the rutile data set (filtering the missing values), distinguishing between grain size (C: coarse, F: fine) and location. Boxplot colors act as a legend for bar-plots. The notch represents a 95% confidence interval on the median The following abbreviations for location have been used: (Ad)-Adirondack; (Cat)-Catskill; (Sha)-Shawangunk; (EGB)-EGB-04-S50; (E2)-EY-29-2; (E3)- EY-29-3; (E4)- EY-29-4. Note that vertical scale of boxplots is in logarithms.

Table 3. Bilateral p-values of the null hypothesis in the equality-of-means tests. The stars show those p-values smaller than: 0.1(*), 0.05(**) and 0.01(***). Tests are applied on the data after replacing missing values by half of the detection limit, and by filtering the samples with missing values. Each sample/location is analyzed separately.

Adirondack	filtered		replaced		EGB-04-S50	filtered		replaced	
ln(V)	0.018	**	0.362		ln(V)	0.004	***	0.030	**
ln(Cr)	0.445		0.749		ln(Cr)	0.001	***	0.016	**
ln(Fe)	0.623		0.028		ln(Fe)	0.185		0.191	
ln(Zr)	0.501		0.512		ln(Zr)	0.008	***	0.066	*
ln(Nb)	0.234		0.012		ln(Nb)	0.149		0.519	
ln(W)	0.395		0.559		ln(W)	0.518		0.026	**
Catskill	filtered		replaced		EY-29-2	filtered		replaced	
ln(V)	$2{\cdot}10^{-5}$	***	$9{\cdot}10^{-5}$	***	ln(V)	0.229		0.303	
ln(Cr)	0.002	***	0.523		ln(Cr)	0.024	**	0.080	*
ln(Fe)	0.460		0.122		ln(Fe)	0.956		0.434	
ln(Zr)	0.001	***	0.174		ln(Zr)	0.657		0.897	
ln(Nb)	0.604		0.105		ln(Nb)	0.044	**	0.124	
ln(W)	0.866		0.251		ln(W)	0.381		0.308	
Shawangunk	filtered		replaced		EY-29-3	filtered		replaced	
ln(V)	0.017	**	0.002	***	ln(V)	0.631		0.986	
ln(Cr)	0.420		0.344		ln(Cr)	0.170		0.163	
ln(Fe)	0.387		0.352		ln(Fe)	0.515		0.632	
ln(Zr)	0.029	**	0.096	*	ln(Zr)	0.226		0.090	*
ln(Nb)	0.419		0.980		ln(Nb)	0.214		0.205	
ln(W)	0.675		0.968		ln(W)	0.009	***	0.029	**
total	filtered		replaced		EY-29-4	filtered		replaced	
V	4		3		ln(V)	0.911		0.733	
Cr	3		2		ln(Cr)	0.849		0.644	
Fe	0		0		ln(Fe)	0.842		0.997	
Zr	4		4		ln(Zr)	0.011	**	0.008	***
Nb	1		0		ln(Nb)	0.313		0.321	
W	2		3		ln(W)	0.002	***	0.004	***

5 Conclusions

Using graphical tools and statistical tests, we confirm in the case of the glacial sediments a strong compositional difference among the four grain-size fractions. Specifically, we detect a clear trend of depletion of Si, Al and Na oxides, as well as enrichment of Mg and Ti oxides with decreasing grain size. The two iron species do not show such a clear-cut trend, but the total $Fe_{(tot)}$ does: in particular, coarse sand and gravel is clearly poorer in $Fe_{(tot)}$ than mud. Finally, there is no significant difference between the composition of the mud and silt (to fine sand) grain-size fractions, except for FeO/Fe_2O_3. Similarly, the contrast between medium sand and coarse sand to gravel is quite low. The strongest contrast is observed between silt (incl. fine sand) and sand (including some gravel/granules). The grain size resolution of the chosen example is not detailed enough to develop a more quantitative picture of the interaction between grain size and glacial sediment chemistry.

Regarding the second example, the chemistry of detrital rutile appears to be not strongly or systematically affected by grain size. Either after removing the samples with zeroes or replacing them, V content appears to be significantly different between the two analyzed grain-size fractions in the Paleozoic sandstone samples (Catskill, Shawangunk). The same holds true, at a lower significance level, for Zr. W plays a discriminative role in two out of three EY (Alpine) samples. Surprisingly, Fe content does not show any significant variation with regard to rutile grain size. In contrast, location and, hence, source rock petrology, exerts a strong control on rutile geochemistry, thus supporting its use as a well-suited tracer mineral for provenance studies. These findings also suggest that trace element composition of rutile has no influence on rutile behavior during weathering, transport, and diagenesis.

This preliminary study on the interactions between sediment and/or mineral composition and grain size plays essentially a confirmatory role regarding prior ideas on the significance of sediment grain size for two particular examples. However, some details are surprising and need further evaluation. The approach also marks a first step towards the study of multi-way compositions (e.g., grain size, chemistry, and mineralogy) which parts admit an array-like structure.

Acknowledgements

We highly appreciate the flexible deadline handling by the CoDaWork comittee. HvE and TZ acknowledge funding by the *Deutsche Forschungsgemeinschaft* (EY23/2, EY23/3, ZA285/2), and RTD those by the *Dirección General de Enseñanza Superior e Investigación Científica* (project BFM2003-05640/MATE, Ministry of Education and Culture, Spanish Government) and the *Direcció General de Recerca* (project 2003XT 00079, *Departament d'Universitats, Recerca i Societat de la Informació, Generalitat de Catalunya*).

References

Aitchison, J. (1986) The Statistical Analysis of Compositional Data. Chapman & Hall Ltd, London (UK) 416p (Reprinted in 2003 with additional material by The Blackburn Press).

Aitchison, J., (1997). The one-hour course in compositional data analysis or compositional data analysis is simple. In: Pawlowsky-Glahn, V. (Ed.), Proceedings of IAMG'97. The Third Annual Conference of the International Association for Mathematical Geology, vol. I, II and addendum. International Center for Numerical Methods in Engineering (CIMNE), Barcelona (E), pp. 3–35.

Gabriel, K.R. (1971) The biplot graphic display of matrices with applications tp principal component analysis. Biometrika, 58: 453-467.

McGill, R., Tukey, J. W. and Larsen, W. A. (1978) Variations of box plots. The American Statistician 32, 12-16. Cited by R Development Core Team (2005, "boxplots.stats" documentation).

Nesbitt, H.W. and Young, G.M. (1996) Petrogenesis of sediments in the absence of chemical weathering: effects of abrasion and sorting on bulk composition and mineralogy. Sedimentology 43, 341-358.

R Development Core Team (2005). R: A language and environment for statistical computing. R Foundation for Statistical Computing, URL: http://www.R-project.org, ISBN: 3-900051-07-0. Vienna, Austria.

von Eynatten H (2004) Statistical modelling of compositional trends in sediments. Sedimentary Geology, 171: 79-89.

Weltje GJ, von Eynatten H (2004) Quantitative provenance analysis of sediments: review and outlook. Sedimentary Geology, 171: 1-11.

Zack T, von Eynatten H, Kronz A (2004a) Rutile geochemistry and its potential use in quantitative provenance studies. Sedimentary Geology, 171, 37-58.

Zack T, Moraes R, Kronz A (2004b) Temperature dependenc of Zr in rutile: empirical calibration of a rutile thermometer. Contributions to Mineralogy and Petrology, 148: 471-488.

Appendix 1: comparison of log- and clr-transformed rutile data set biplots

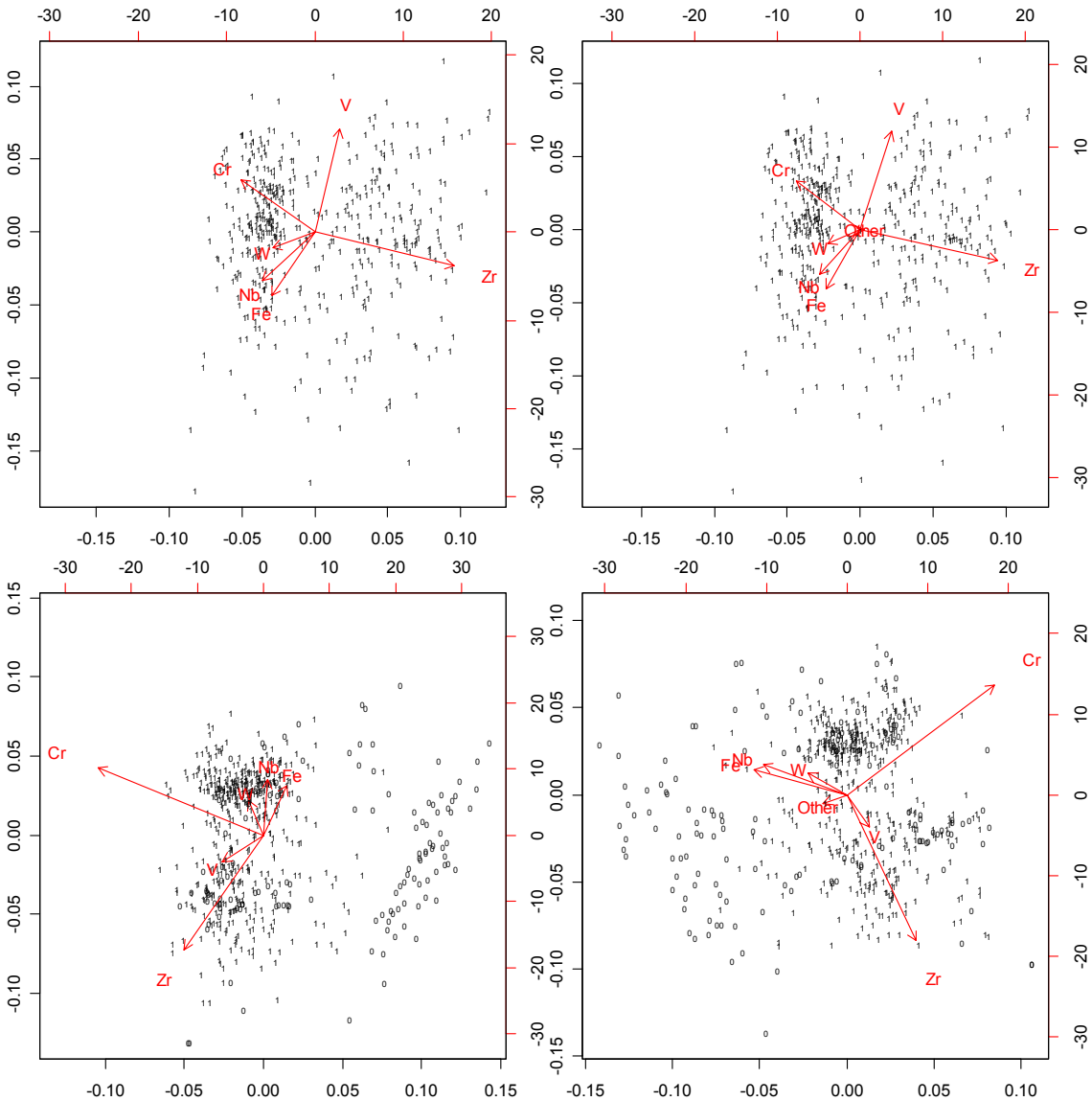

Figure 7: Biplots of the whole rutile data set. Missing values are marked with "0", whereas fully observed compositions with "1": (upper) filtering the missing values; (lower) replacing the missing values by half of its detection limit; (left) taking log-transformed variables, (right) taking clr-transformed variables, including the residual part as "Other".

Appendix 2: a first dip in a log-linear modelling of the glacial sediment data set

True two-way compositions may be related to two-way contingency tables. A contingency table is the result of counting how many times the intersection of all possible levels of two categorical variables occurs. Contingency tables can be analyzed using log-linear models (e.g., Simonoff, 2003). Let X_1 and X_2 represent the two categorical variables, respectively with I and J levels. Let n_{ij} represent the number of times we observed $X_1=i$ and $X_2=j$, with $1\leq i \leq I$ and $1\leq j\leq J$, and p_{ij} be the probability of occurrence of that event. Let $p_{i\cdot}$ and $p_{\cdot j}$ represent the marginal probabilities of $X_1=i$ and $X_2=j$ respectively (with the dot indicating summation by the replaced index). Denote by n the total number of observations. It is well-known that the expectation of $\mathrm{E}[n_{ij}]= np_{ij}$. Also, if X_1 and X_2 are independent, this implies that $p_{ij} = p_{i\cdot}p_{\cdot j}$, which means that $\mathrm{E}[n_{ij}] = n\cdot\, p_{i\cdot}p_{\cdot j}$. Taking logs of these expressions we get in general,

$$\log \mathrm{E}\left[n_{ij}\right] = \log n + \log p_{ij} = \lambda_0 + \log p_{ij}$$

If we assume independence of the two categorical variables, we obtain

$$\log p_{ij} = \log p_{i\cdot} + \log p_{\cdot j} = \lambda_{i\cdot} + \lambda_{\cdot j},$$

involving the so-called *row and column effects*, respectively denoted by $\lambda_{i\cdot}$ and $\lambda_{\cdot j}$. Since there are many sets of $\{\lambda_{i\cdot}\}$ and $\{\lambda_{\cdot j}\}$ giving the same probabilities, one classically selects those which sum up to zero. This implies that these row and column effects can be computed as the clr transformations (4) of the marginal probability vectors. Finally, if independence is not desired, one can add an *interaction effect* between row i-th and column j-th, denoted by λ_{ij}, which gives

$$\log p_{ij} = \lambda_{i\cdot} + \lambda_{\cdot j} + \lambda_{ij}\,.$$

If a perfect fit is sought, interactions can be computed as

$$\lambda_{ij} = \log \frac{p_{ij}}{p_{i\cdot}p_{\cdot j}}\,. \tag{5}$$

However, this would mean that we would use $I+J+I\cdot J$ parameters to describe a table of $I\cdot J$ numbers (with $I\cdot J-1$ degrees of freedom, due to the closure). The usual application of log-linear models is not to get this perfect fit, but to structure a set of tests of independence (levels i-th and j-th are independent if we accept the null hypothesis $\{\lambda_{ij}=0\}$) or assume parsimonious models for interactions, and estimate its parameters. We will consider an interaction model which takes into account that one of our categories (e.g., grain size, say, by columns) is ordered. In this case, interactions are computed with the model

$$\lambda_{ij} = \tau_i\left(v_j - \overline{v}\right), \tag{6}$$

where $\{v_j\}$ are previously-specified values for all j-th levels of the column variable (e.g., in our grain size, they will be $v_j=j$, and $\overline{v} = -2.5$ is their mean), and $\{\tau_i\}$ are the I model parameters to estimate.

As we explained in the first section of this contribution, we have no true two-way compositions, but classical geochemical compositions with an additional record of grain size. Thus, we first construct a two-way composition representing the mean of the glacial sediment data set, which we will afterwards model with log-linear techniques. To do so, we compute the center (=closed geometric mean of parts) of the composition for each grain size, and each center is multiplied by a weight proportional to the number of observations in that grain size (Table 4). Thus, each cell of Table 4 contains p_{ij} the proportion *of* the i-th chemical species *of* the j-th grain fraction *in* the whole composition (equivalent to a joint probability). This has been indirectly obtained as $p_{ij} = m_{i|j}\cdot p_{\cdot j}$, being $m_{i|j}$ the computed mean proportion *of* the i-th chemical species *in* the j-th grain fraction (equivalent to a conditional probability). Then, interaction effect are computed using equation (5), which gives

$$\lambda_{ij} = \log \frac{p_{ij}}{p_{i\cdot}p_{\cdot j}} = \log \frac{m_{i|j}p_{\cdot j}}{p_{i\cdot}p_{\cdot j}} = \log \frac{m_{i|j}}{p_{i\cdot}} = \log \frac{m_{i|j}}{\sum_j p_{\cdot j}m_{i|j}}$$

These effects are plotted in Figure 8(A), and they can be interpreted as the log-ratio of the mean of each grain size against a given global mean. This global mean is a weighted arithmetic mean of the means of all grain-sizes, which is a strange mixture of geometric and arithmetic criteria. Instead, we could have chosen the global closed geometric mean (denoted: m_i), ignoring grain size differences. This gives an estimate of the interaction effects equal to

$$\lambda_{ij} = \log \frac{m_{i|j}}{m_i}\,.$$

This second way of estimating interaction effects was used to obtain Figure 8(B). These two figures are barely distinguishable (as are the two last columns of table 4, containing $p_{i\cdot}$ and m_i), implying that the global geometric mean and the mixed geometric-arithmetic mean are surprisingly almost equal.

Table 4: Constructed two-way mean composition of the glacial sediments.

$X_1=i$	$X_2=j$ / v_j	mud 1	silt to fine sand 2	medium sand 3	coarse sand to gravel 4	marginal composition	m_i compositional mean (global)
SiO_2		$2.78\cdot10^{-1}$	$1.13\cdot10^{-1}$	$1.63\cdot10^{-1}$	$1.33\cdot10^{-1}$	$6.88\cdot10^{-1}$	$6.88\cdot10^{-1}$
TiO_2		$2.86\cdot10^{-3}$	$1.00\cdot10^{-3}$	$8.38\cdot10^{-4}$	$6.12\cdot10^{-4}$	$5.31\cdot10^{-3}$	$5.16\cdot10^{-3}$
Al_2O_3		$6.15\cdot10^{-2}$	$2.42\cdot10^{-2}$	$3.23\cdot10^{-2}$	$2.75\cdot10^{-2}$	$1.46\cdot10^{-1}$	$1.46\cdot10^{-1}$
Fe_2O_3		$1.30\cdot10^{-2}$	$4.45\cdot10^{-3}$	$5.31\cdot10^{-3}$	$3.42\cdot10^{-3}$	$2.62\cdot10^{-2}$	$2.60\cdot10^{-2}$
FeO		$1.12\cdot10^{-2}$	$4.35\cdot10^{-3}$	$3.70\cdot10^{-3}$	$2.33\cdot10^{-3}$	$2.16\cdot10^{-2}$	$2.10\cdot10^{-2}$
MgO		$1.11\cdot10^{-2}$	$3.89\cdot10^{-3}$	$3.70\cdot10^{-3}$	$2.59\cdot10^{-3}$	$2.13\cdot10^{-2}$	$2.09\cdot10^{-2}$
CaO		$1.39\cdot10^{-2}$	$5.34\cdot10^{-3}$	$6.98\cdot10^{-3}$	$5.07\cdot10^{-3}$	$3.13\cdot10^{-2}$	$3.14\cdot10^{-2}$
Na_2O		$1.32\cdot10^{-2}$	$5.55\cdot10^{-3}$	$8.19\cdot10^{-3}$	$7.25\cdot10^{-3}$	$3.42\cdot10^{-2}$	$3.40\cdot10^{-2}$
K_2O		$1.09\cdot10^{-2}$	$4.15\cdot10^{-3}$	$4.94\cdot10^{-3}$	$5.01\cdot10^{-3}$	$2.50\cdot10^{-2}$	$2.50\cdot10^{-2}$
P_2O_5		$9.03\cdot10^{-4}$	$3.40\cdot10^{-4}$	$2.95\cdot10^{-4}$	$2.07\cdot10^{-4}$	$1.75\cdot10^{-3}$	$1.71\cdot10^{-3}$
marginal granulometry		$4.17\cdot10^{-1}$	$1.67\cdot10^{-1}$	$2.29\cdot10^{-1}$	$1.88\cdot10^{-1}$	1.00	1.00

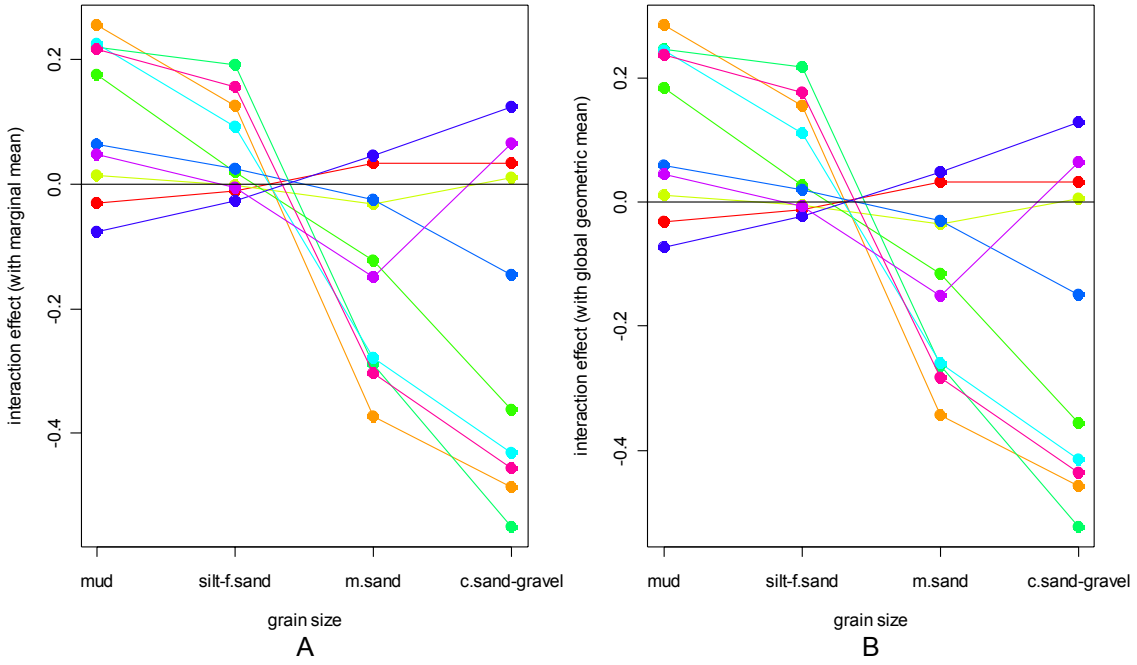

Figure 8: interaction effects grainsize-geochemistry, computed: (A) with the marginal mean composition (mixed geometric-arithmetic approach), (B) with the global compositional mean (purely geometric approach). Codes of colours follow Figure 2.

Figure 8 clearly shows a decreasing trend from mud to gravel for Fe_2O_3 (bright green), FeO (bluish green), TiO_2 (orange), P_2O_5 (magenta) and MgO (cyan blue). Subtler trends are also observed for CaO (electric blue, decreasing), and Na_2O (dark blue, increasing), even for SiO_2 (red, slightly increasing). Finally, lacking a true test of independence, Al_2O_3 proportion (yellow) presents a fairly flat and null interaction effect with grain size. K_2O (violet) pattern is much complex: it might either be interpreted as a preferential depletion in sand out of a fairly independent behaviour with grain size, or as a preferential enrichment of K_2O in coarser grains with respect to a general decreasing trend. In the other cases, the good similitude of the dots with true straight lines is a very promising result. Note that we can also observe here the anomalous high FeO content (bluish green) in silt and fine sand. These increasing or decreasing trends are also clear after estimating the τ_i parameters of a model attending to the ordering of grain size (Eq. 6). Each of these lines was obtained by regression of the four dots in Figure 8 forcing a zero intercept, and they are all summarized in table 5.

Table 5: slope parameters of the ordered-categories model.

$X_1=i$	SiO_2	TiO_2	Al_2O_3	Fe_2O_3	FeO	MgO	CaO	Na_2O	K_2O	P_2O_5
τ_i	0.0237	-0.2726	-0.0042	-0.1758	-0.2790	-0.2343	-0.0677	0.0676	-0.0088	-0.2477